Paper 4

Impact of deltaic clinothems on reservoir performance: dynamic study of reservoir analogues from the Panther Tongue and Ferron Sandstone, Utah, USA.

Håvard D. Enge[1,2] and John A. Howell[2]

[1]*Department of Earth Science, University of Bergen, Box 7800, 5020 Bergen, Norway*

[2]*Centre for Integrated Petroleum Research, University of Bergen, Box 7800, 5020 Bergen, Norway*

Corresponding author: havard.enge@cipr.uib.no

Abstract

Subsurface reservoir models are typically limited by a lack of spatially accurate geometric data on bedform architecture and geometry, which are key controls on fluid flow. Outcrop analogues have long be utilized as a source of such data, but the capture of sufficiently precise data has always been a challenge.

This study utilizes three-dimensional, high-resolution, digital geological outcrop data generated by ground-based laser scanning (lidar) to build three-dimensional (3D) geocellular models of two well exposed ancient river-dominated delta systems that both crop out in central Utah, USA. The forced regressive Panther Tongue and a high-stand portion of the Ferron Sandstone have been digitally mapped to recreate their clinothem geometries in geocellular reservoir modelling software for the testing of simulated production of such clinothem systems.

Clinothems are seaward dipping beds of the delta front, formed during the downstream accretion of the delta. Clinoforms separate the deltaic sandbody into a series of sandstone beds (clinothems) which are commonly draped with siltstones and mudstones that within a reservoir may significantly impact fluid flow

The models are used to test the influence of dipping siltstones heterogeneities on simulated reservoir performance in the reservoir modelling software. Siltstone drapes on clinothem sandstone beds have been modelled and various populations of holes have been placed in the siltstone beds (0, 30, 60, 90 and 100%). The effects of siltstone permeability (1, 0.1, 0.01 and 0.001 mD) have also been tested. A total of 41 individual models were built and flow simulated.

Results quantify how the portion of holes governs the production rate/ recovery factor in the Panther Tongue models. Permeability values are more important in the Ferron models, although they are still influenced by the number of holes. Steeper dipping and closer spaced clinothems of the highstand system tract lower the recovery factor by several tens of percent if the related heterogeneities are all or close to continuous and have low enough permeability.

Introduction

Shallow marine systems act as significant and potentially heterogeneous hydrocarbon reservoirs in many parts of the world. Within a single field, heterogeneities can occur at a variety of scales from the pore to the sequence (e.g. Weber, 1986; Weber and van Geuns, 1990; Kjonsvik et al., 1994). Many of the scales lie in the "scale gap" between the well and seismic databases which form the main sources of information on the occurrence, distribution and geometries of heterogeneities. At this point the utilization of data, models and dynamic interrogation (flow simulation) of analogous outcrops can contribute significantly to understanding reservoir performance (e.g. Dreyer et al., 1993; White and Barton, 1999; Howell et al., 2008).

Deltaic systems commonly contain dipping clinoforms (Bhattacharya and Walker, 1992). Clinoforms are surfaces that represent the palaeo-position of the delta front surface as it prograded (Rich, 1951). Clinoforms separate the deltaic sandbody into a series of sandstone beds (clinothems) which are commonly draped with siltstones and mudstones. The presence of these dipping shale layers within a reservoir may significantly impact both horizontal and vertical fluid flow, yet they are rarely included in subsurface reservoir models. (e.g. Ainsworth et al., 1999; Tye et al., 1999; Willis and White, 2000; Bhattacharya and Willis, 2001; Howell et al., 2008; Skorstad et al., 2008; Howell et al., in press)

The aim of the present study is to build three-dimmensional (3D) geocellular models of two well exposed outcrops of deltaic sandstone and recreate the clinothem geometries which have been digitally mapped in the field. These models have been built at a scale that is analogous to the inter-well spacing in a typical offshore hydrocarbon field (several hundred meters) and which sufficiently captures several tens of clinothems and associated dipping barriers. This scale also fills the gap between laterally restricted, core and, low resolution, seismic data. The models capture the individual bed geometries and have been flow simulated to investigate the controls on reservoir performance The building and testing of small-scale, outcrop based, geocellular analogue models is an established method for representing and investigating subsurface reservoirs (e.g. Bryant and Flint, 1993; Dreyer et al., 1993; Froster et al., 2004; van den Bergh and Garrison, 2004; Enge et al., 2007; Rotevatn et al., 2007; Labourdette et al., 2008).

A common challenge to building accurately constrained reservoir models from outcrops has been the capture and representation of the geological outcrop with sufficient precision. This issue has been addressed by the collection of high-resolution 3D, digital data from outcrops (c.f. Enge et al., 2007). A ground-based laser scanner (lidar) has allowed for the rapid collection of spatially accurate geometric data, the building of accurate virtual outcrops and the interpretation of large volumes of geological data. The use of lidar is now an established and well tested method for capturing outcrop data (e.g. Olariu et al., 2005; Buckley et al., 2006; Pringle et al., 2006; Enge et al., 2007; Redfern et al., 2007; Buckley et al., 2008; Enge et al., Submitted-b; Enge et al., Submitted-a).

A workflow which covers all of the steps from collecting outcrop data to performing full scale reservoir flow simulation has been described by Enge et al. (2007). Virtual outcrop models have been created from two well exposed river-dominated deltaic successions, the lower part of the Ferron Sandstone which crops out around Ivie Creek, and the Panther Tongue which outcrops near the town of Helper, both in central Utah (Fig. 1). These virtual outcrop models have been used to extract detailed bed statistics which describe the morphology of the clinothems (Enge et al., Submitted-b; Enge et al., Submitted-a). In the current presentation, the same virtual outcrop models have been used to build detailed geocellular models to test the controls on simulated fluid flow.

The outcrop-based, geocellular models have been built from surfaces mapped from the virtual outcrop models. Dynamic testing has been used to look at the effects of the dipping shale-draped clinoform surfaces on fluid flow. Specifically the models have been used to test the influence of the barriers; the effects of holes, caused by erosion of the siltstone layers and, variations in siltstone permeability on simulated production. In addition, the modelled portions of the Panther Tongue and Ferron Sandstone both contain clinoforms but with different geometries. These different geometries (discussed further below) have been interpreted to result from different accommodation regimes at the time of deposition (Jervey, 1988; Posamentier et al., 1988; Pirmez et al., 1998); thus the effects of clinothem geometry systems tract on fluid flow can be compared and contrasted.

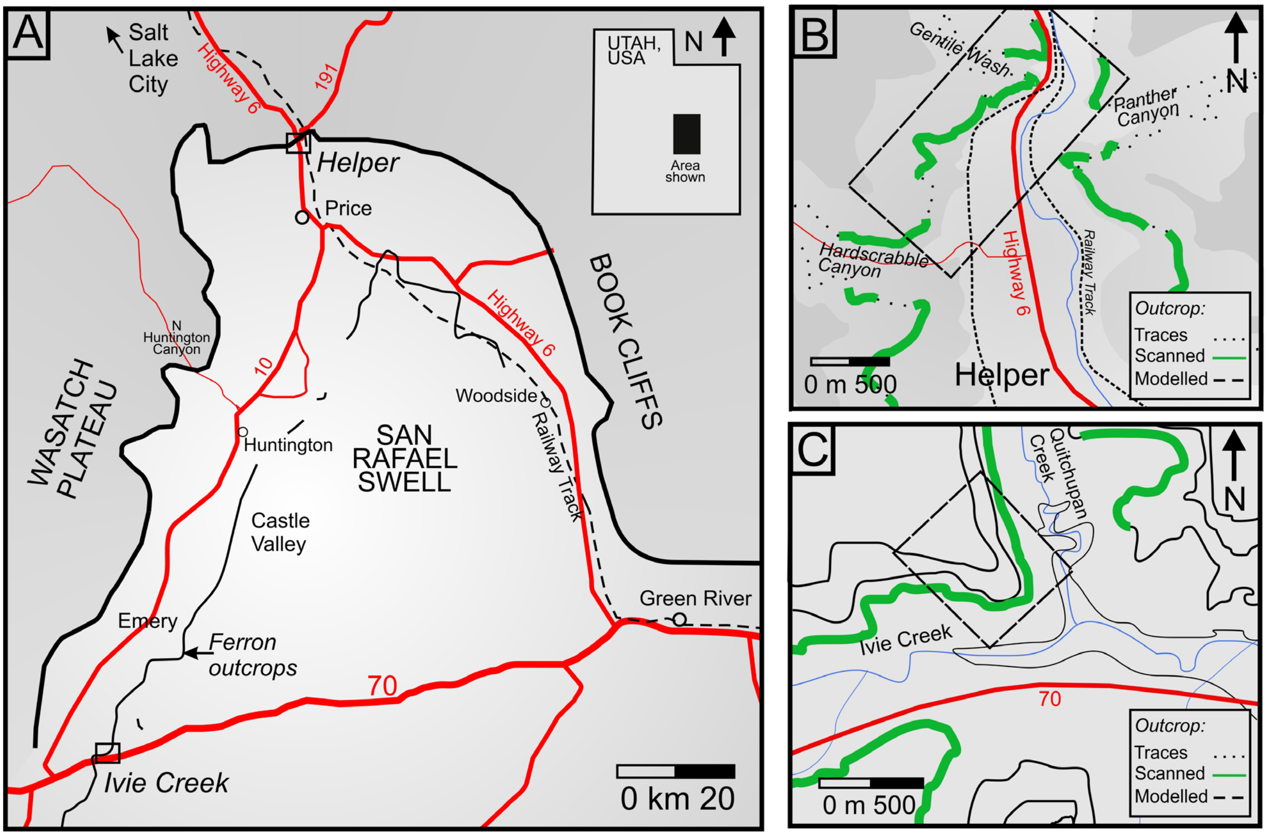

Fig. 1. Study areas. **(A)** Central Utah with location of the two study areas. **(B)** The Helper area with the Panther Tongue outcrops. **(C)** Ivie Creek area with the Ferron Sandstone outcrops. Modelled areas are outlined in B and C.

Clinoforms and clinothems: a summary

Clinothem beds result from deposition on the dipping, seaward side of a mouth bar complex. Rich (1951) used the term clinoform to describe surfaces that represent the palaeo position of the delta front surface and clinothem to describe the body of sediments or rock bounded by individual clinoforms. Distal mouthbar clinothems occur as beds that dip, thin and fine in a seaward direction in an en-echelon pattern (Howell et al., 2008), normally deposited from turbidity currents in the delta front (Posamentier and Morris, 2000; Olariu et al., 2005; Catuneanu, 2006). Clinothem beds may contain a variety of interfingering facies (e.g. Gani and Bhattacharya, 2005), and sand rich portions of the beds are commonly interbedded with siltstone beds that were deposited during quieter periods (Posamentier and Morris, 2000; Bhattacharya and Davies, 2001; Anderson et al., 2004). In outcrop, the finer material typically occurs as recessive breaks in the cliff face.

Deposition in deltas commonly occurs at the mouth of terminal distributary channels where mouth bars and amalgamated mouth bar complexes are formed (Postma, 1990; Olariu and Bhattacharya, 2006). Autocylic avulsion of both the channel and the mouth bar complex causes progradation of mouth bar successions and formation of new delta lobes. In this and related studies (Enge et al., Submitted-b; Enge et al., Submitted-a), packages of sediment with genetically related clinothems are termed bedsets (sensu Van Wagoner et al., 1990). These bedsets equate to the individual, autocyclically derived delta lobes (see Enge et al., Submitted-b; Enge et al., Submitted-a for a full discussion).

Geological overview

The studied intervals both crop out in central Utah (Fig. 1). The first case study is from the normally regressive, highstand Ferron Kf-1 parasequence set of the Ferron Member that crops out in the Ivie Creek area near Interstate 70, Utah (Ryer, 1981; Ryer and Anderson, 2004). The second system studied is the forced regressive, falling to lowstand system tract Panther Tongue Member that crops out in the area around Helper, Utah (Young, 1955; Howard, 1966; Newman and Chan, 1991; Posamentier and Morris, 2000). Both systems were laid down on the western edge of the Cretaceous interior seaway which occupied a foreland basin that developed as a result of flexural down-warping of the lithosphere due to the rise of the Sevier Orogenic belt in the west (Jordan, 1981; Fouch et al., 1983; Kauffman, 1984; Cross, 1986). Further details of the regional geology are discussed in Enge et al. (Submitted-b; Submitted-a).

The Ferron Member of the Mancos Shale Formation

In outcrop the Turonian-aged Ferron Member extends for over 70 km along the western flank of the San Rafael Swell. An area of more than 2 km² in the Ivie Creek site comprises a continuous buttress up to 20 m high, with a close to depositional dip view on two sides and a more strike-oriented section at the southern end (Fig. 1C). The present study has focused on the lower most upward-coarsening succession in the buttress termed Kf-1-Ivie Creek[a] by previous workers (Anderson and Ryer, 2004; Garrison and van den Bergh, 2004). Kf-1-Ivie Creek[a] has a depositional dip extent of about 2.4 km, is conformably underlain by the offshore Tununk shale and overlain by the bedset Kf-1-Ivie Creek[c] (Anderson et al., 2004). It prograded towards the north and northwest in an embayment sheltered from waves during a highstand in relative sea-level (Anderson et al., 2004; Garrison and van den Bergh, 2004;

Mattson and Chan, 2004). Kf-1-Ivie Creek[a] is a part of Kf-1 which is composed of multiple stacked and laterally extensive mouth-bar deposits, indicating strong river influence (Gardner et al., 2004; van den Bergh and Garrison, 2004). In the study area, Kf-1-Ivie Creek[a] contains numerous northward-dipping clinothem beds which are predominantly fine to medium grained (Mattson and Chan, 2004) and are interbedded with siltstone which pinch out in an updip direction (Fig. 2A). The studied interval includes three bedsets (Enge et al., Submitted-a).

The Panther Tongue Member of the Star Point Formation

The Campanian-aged Panther Tongue is exposed along the eastern flank of the Wasatch Plateau and in the western limit of the Book Cliffs (Young, 1955; Howard, 1966). The focus of this study has been a 2 km² area with a 25 m high outcrop section slightly north of the town of Helper, west of Highway 6 between Gentile Wash and Hardscrabble Canyon, which comprises a close to depositional dip section (Fig. 1B). Interpretations from the entrance to the Panther Canyon east of Highway 6, have also been used.

In vertical section the Panther Tongue typically shows an upward coarsening and upward cleaning profile with an increase in sandstone bed thickness. The basal bounding surface of the Panther Tongue is a gradual transition from the underlying Blue Gate Shale (Posamentier and Morris, 2000; Catuneanu, 2006), and it is capped by a regional transgressive lag (Newman and Chan, 1991; Hwang and Heller, 2002). The Panther Tongue lacks time equivalent coastal plain deposits (Posamentier and Morris, 2000; Olariu et al., 2005; Howell et al., 2008), and is interpreted as a falling to lowstand delta.

Sandstone clinothems in the Panther Tongue are typically fine grained with thin (10 - 20 cm) siltstone interbeds seen as recessive breaks in the outcrop (Fig. 2B). The clinothem beds generally dip palaeo-seawards, are thickest in the proximal parts and become thinner basinward before they eventually pinch out in the underlying Mancos shale in an offlapping manner. Four bedsets have been mapped in the study area (Enge et al., Submitted-b; Enge et al., Submitted-a), of which the stratigraphically lowermost has been the focus of this study.

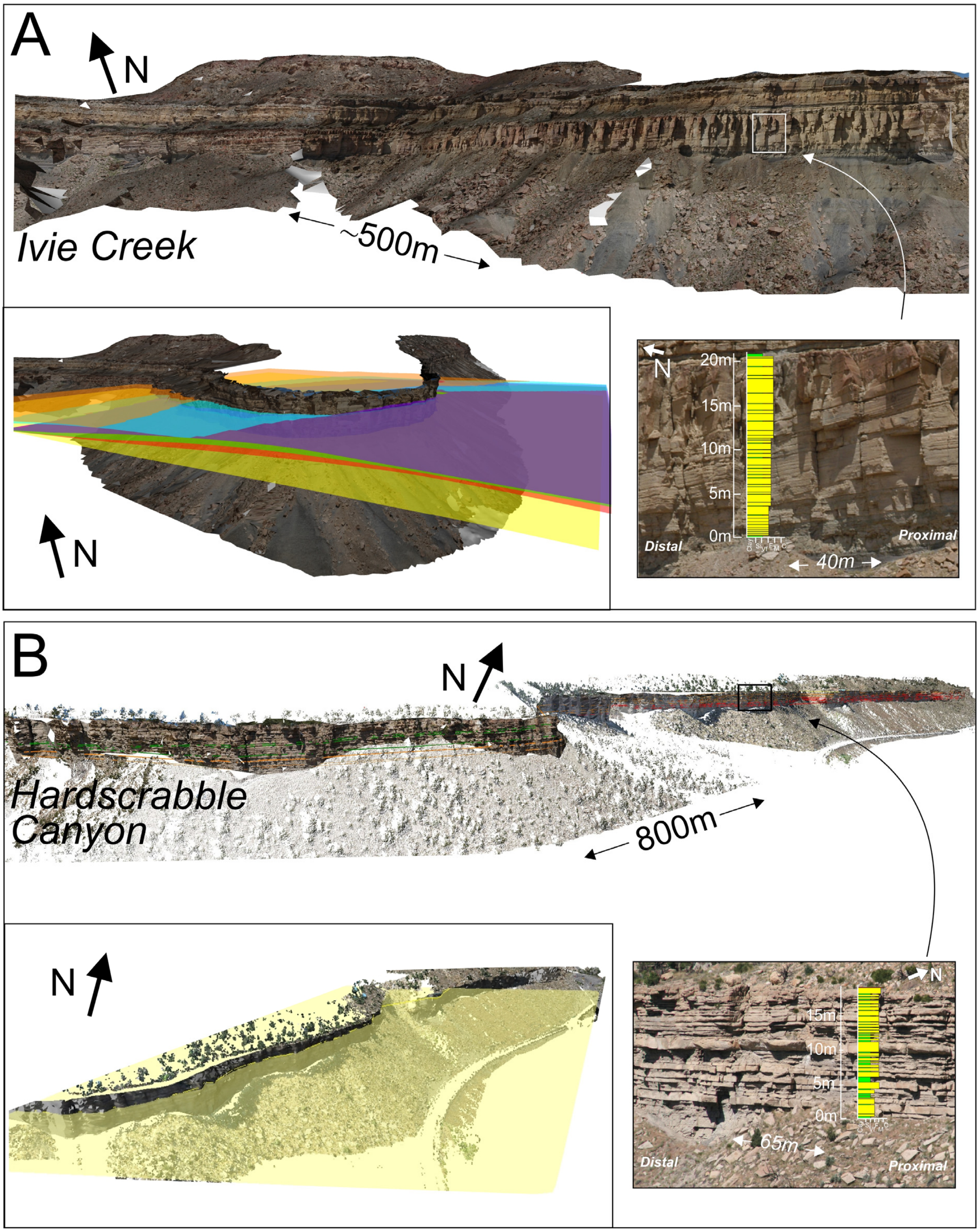

Fig. 2. Virtual Outcrop Models (VOMs) examples and schematic lithological logs from the study areas. Inserts show VOMs together with surfaces used to delineate zones in reservoir modelling. **(A)** Ivie Creek area of the Ferron Sandstone. **(B)** The area between Gentile Wash and Hardscrabble Canyon of the Panther Tongue study area.

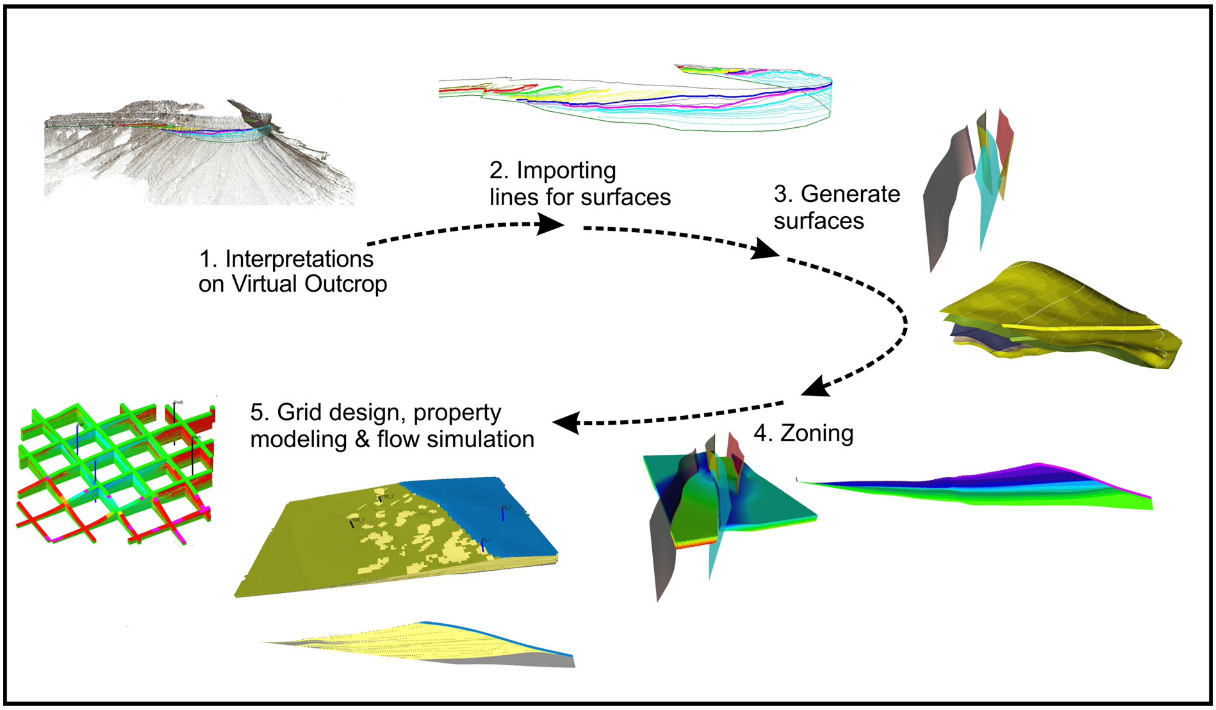

Fig. 3. Workflow showing the steps involved from acquiring the outcrop data to building and flow simulation of reservoir models. See text for details. After Enge et al. (2007).

Field methods

The steps involved in acquiring the outcrop data and the generation of virtual outcrop models are outlined at length in Enge et al. (2007) and Buckley et al. (2008). Details of procedures for extraction of surface (bed) data in the virtual outcrop, export of data from the virtual outcrop and import of data into reservoir modelling software are outlined in Enge et al. (2007), with additional examples in (Rotevatn et al., in press). The workflow is summarised in figure 3. A brief review is given below.

Traditional field methods were used as a complementary method to laser scanning to collect data on grain size and bed characteristics that are below the resolution of the scanner. Petrophysical data for the flow simulation were not collected from the field. These were assigned later on a facies by facies basis (see below).

Input from virtual outcrop to reservoir models

The morphology of the outcrop is captured in detail by ground-based laser scanning (lidar). The scanner collects the XYZ position of millions of points on the outcrop. This point cloud is decimated and then triangulated to recreate the outcrop surface. The triangles are textured with digital photos collected with the points; the resultant textured surface is the virtual outcrop model (VOM)(Fig. 4) (Enge et al., 2007; Buckley et al., 2008). Within the VOM each pixel has an XYZ position that is typically accuracy of better than +/- 10 cm. The VOM can be visually interrogated and points and polylines that represent key geological surfaces can be digitized. Once mapped and interpreted in three dimensions, the points and polyline data can be exported to a reservoir modelling software which in the current study was Roxar's Irap RMS v 9.05 (Enge et al., 2007; Roxar, 2008). Once in the modelling software the points and polylines can be extrapolated to recreate the geological surfaces in 3D (Fig. 4). Figure 4B illustrates examples of such surfaces viewed together with the VOM. The volume between these surfaces is then subdivided into grid cells which are in turn assigned facies and petrophysical properties. Wells are placed in the model and the flow of fluid is numerically simulated.

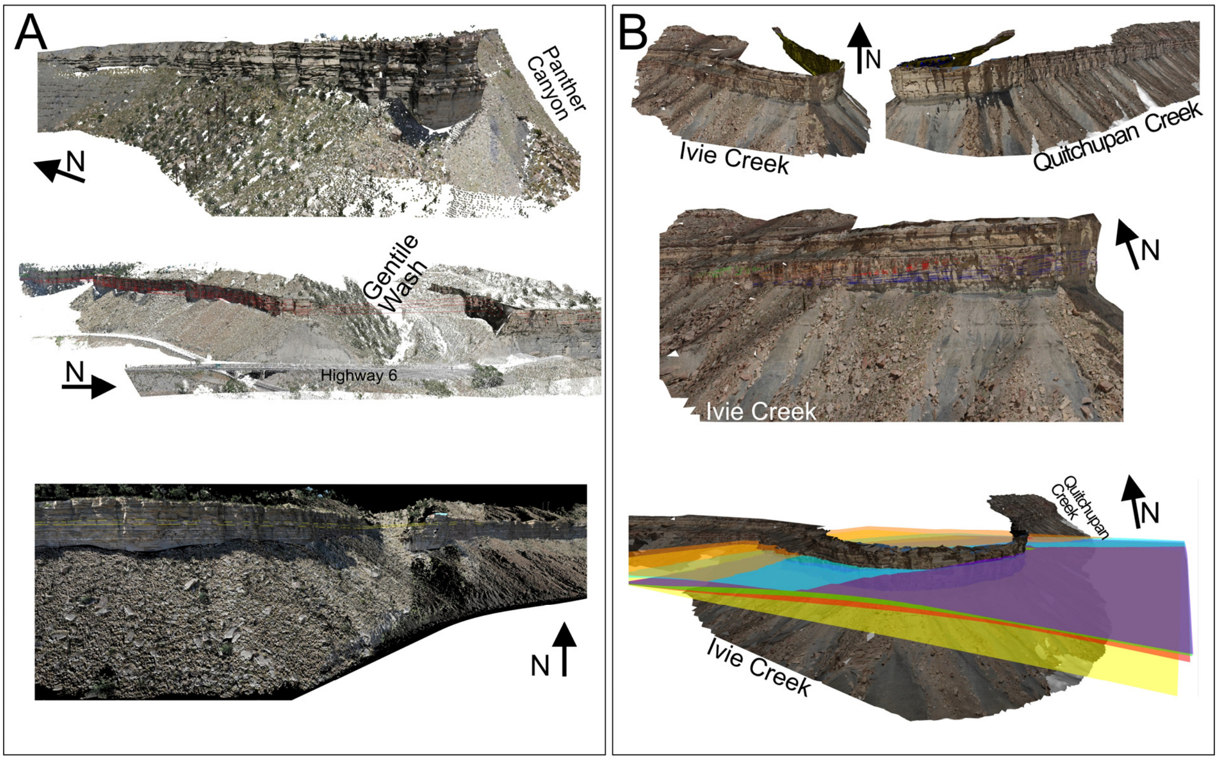

Fig. 4. Examples of virtual outcrop models (VOMs) from the study areas. Interpretations are done directly in the VOMs and used to created surfaces for reservoir modelling. **(A)** Panther Tongue. **(B)** Ferron Sandstone.

Reservoir Modelling

A reservoir model is a computer-based 3D quantitative representation of a volume of rock. The volume is divided into cells which are assigned properties which reflect the geology; consequently, such models are commonly referred to as geocellular models. In addition to geological information, cells may also be populated with petrophysical data (porosity, permeability vectors, fluid saturations etc). Reservoir modelling is an important part of predicting, planning and updating information concerning subsurface hydrocarbon reservoirs. As a database it includes geological, petrophysical and production data. A geocellular model of an outcrop provides a framework for recreating the outcrop in 3D, capturing its geometry and addressing issues that control fluid flow which cannot be determined from subsurface data alone.

Rationale

The number of cells in a model is limited by the computing power available. The size of the individual grid cells is therefore limited by the total volume to be modelled. Grid resolution is controlled by the modeller and may vary through the model. The final grid size will depend upon the scale of heterogeneities to be captured, the purpose of the model and the trade-off between detail and speed. A typical cell in a subsurface simulation model is 50-200 m in the horizontal direction and 1-5 m in the vertical resolution (e.g. Howell et al., 2008). It is recognised that significant heterogeneities may occur within such a volume and these are typically captured by upscaling studies (Stephen et al., 2008). Such studies may address issues from the pore, through the bedform to the facies and facies association scale (Stephen et al., 2008). One method of upscaling is to build more detailed models that are designed to capture the detail of the heterogeneity to be considered. Such models should be designed to capture the representative elemental volume.

In this study "close to deterministic" models with a high number of smaller cells have been built from analogue rock volumes that capture the detail of the dipping clinothems. The models include several hundred thousand cells with a typical resolution of 1 x 1 x 0.2m. Two base-case models were built, one for the Panther Tongue and one for the Ferron. From these base-cases a series of child models were created to investigate issues related to the effects of dipping clinothem beds, bedset geometries and varying flow-properties (permeability) and coverage of silt drapes on the clinoforms. The present study recognizes heterogeneities that represent potential barriers to fluid flow at two different scales: 1) bed or clinothem, 2) bedsets or mouthbar / lobe. Whilst both are related to the presence of dipping silt barriers within the delta front sandstone, the latter may also be associated with a significant change of outbuilding direction, a change of clinothem dip and the possibility for reservoir to be juxtaposed with non-reservoir.

The clinothem geometry and architecture were captured from the VOM and recreated “close to deterministically” for the base-case models. Two parameters related to the siltstone beds that drape the clinoforms were not measured from the outcrop. The first is the continuity of the siltstone beds and the distribution of holes, formed shortly after deposition by erosion during the subsequent flow event. A suite of five models ranging from 0% holes (total coverage) to 100% holes (no shale layer present) were built to address the range of possible values. The second parameter was the permeability of the shale layers, which in part reflects the grain size and sorting of the siltstone drapes. Four different values were modelled, 0.001, 0.01, 0.1 and 1 mD (see Table 1). A matrix of models was built to investigate the relative importance of these two parameters (Fig. 5). The quantitative and qualitative results of the simulations can potentially be used to provide more constrained values for the coarser cells in full field models.

Table 1. Matrix of flow simulated models. The matrix gives a total of 40 models, 20 from the Panther Tongue and 20 from the Ferron Sandstone. In addition, one Ferron model with extra bedset-barriers raises the total number of models to 41.

Siltstone/lag permeability Model	**Kv / Kh (mD)**	**Kv / Kh (mD)**	**Kv / Kh (mD)**	**Kv / Kh (mD)**
0 % holes	1	0.1	0.01	0.001
30 % holes	1	0.1	0.01	0.001
60 % holes	1	0.1	0.01	0.001
90 % holes	1	0.1	0.01	0.001
100 % holes	1	0.1	0.01	0.001
ALL models:	Kv/Kh sandstone 1.95/90 mD. Porosity siltstone and lag 0.05; sandstone 0.25.			

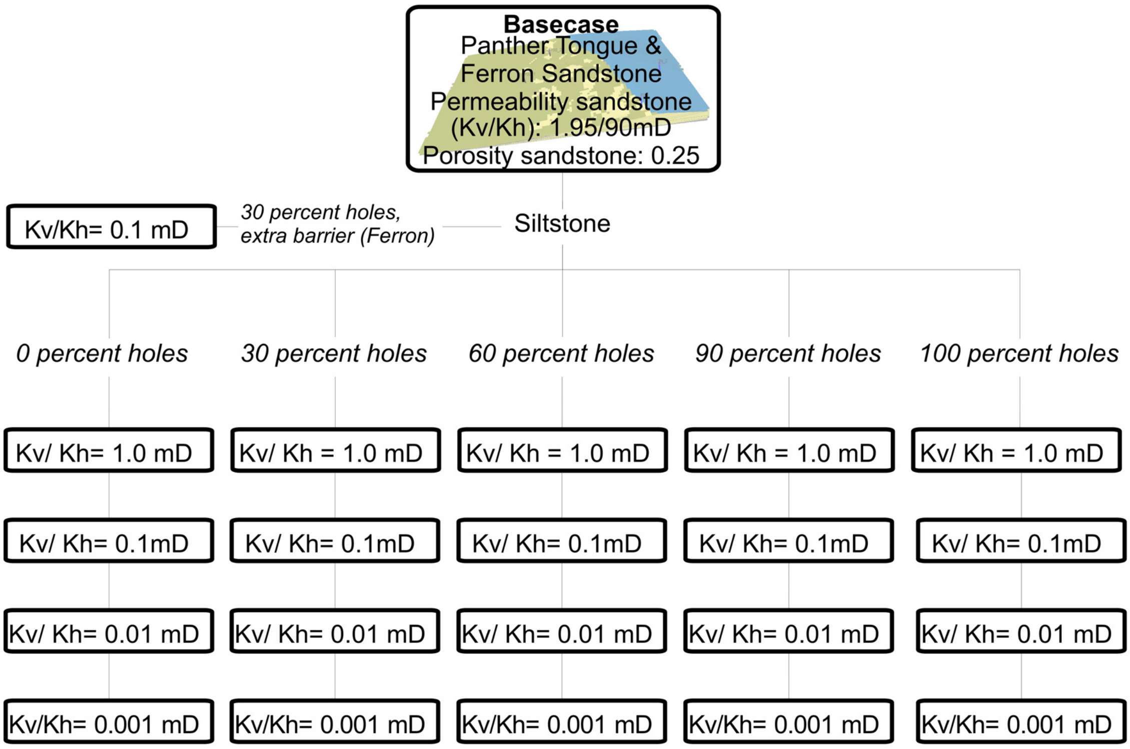

Fig. 5. Experimental design. The set up is identical for the two modelled areas, but with an addition of one model with extra bedset-barriers from the Ferron Sandstone. In total, this gives 21 and 20 different models from the Ferron Sandstone and the Panther Tongue, respectively.

Model building: The surface-based framework

Digitised clinothem bed boundaries represented by a series of closely spaced points were imported from the VOM into RMS. Unlike interpreted surfaces from 3D seismic data which are normally used to create a model, the points and polylines that represent the virtual outcrop expression of a clinothem are not in themselves continuous surfaces; they only represent a small part of the surface where it intersects the topography. The surfaces need to be regenerated from the points and polylines through extrapolation. RMS contains a variety of algorithms for the extrapolation of surfaces. Continuous exposure, with a high outcrop area ratio (Enge et al., 2007), as is the case with both of the chosen outcrops, greatly enhances the accuracy of the extrapolated surfaces. Visual quality check and comparison with the geological outcrop is used to determine whether the algorithms are producing the optimal resemblance to the clinothems. Since the Z values derived from the virtual outcrop are heights above sea-level and the modelling software typically uses “depth below surface”, the entire project was translated to typical shallow reservoir depth (c. 1000 m).

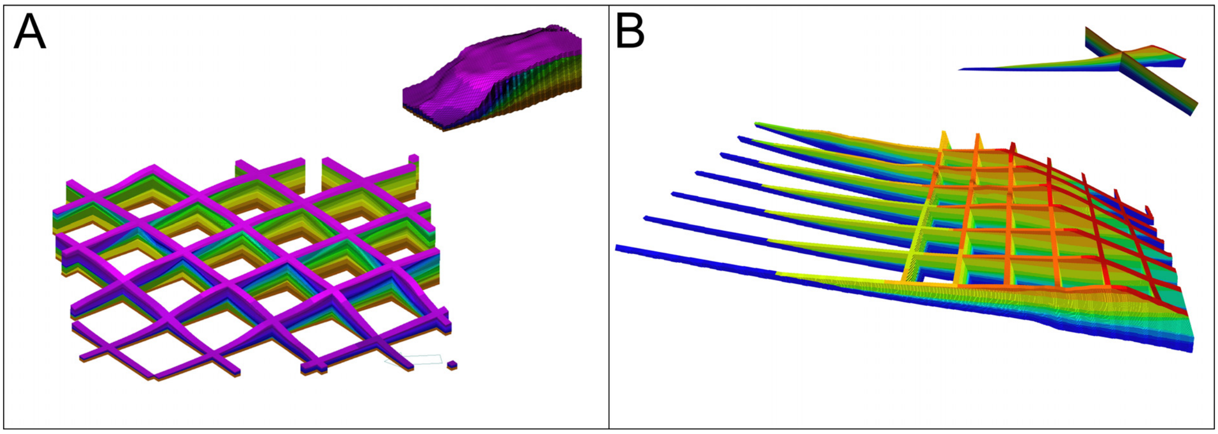

Fig. 6. Modelling zones shown in different colours. In the models built, each single clinothem is represented by a separate zone. **(A)** The Ferron Sandstone model with 37 surfaces, representing 35 clinothems in three bedsets and one basal zone. **(B)** The Panther Tongue contains a total of 14 surfaces representing 13 clinothems within a single bedset.

The model surfaces form the framework for the grid which contains the properties. In the Ferron Sandstone model 37 surfaces were included in the final model, representing 35 clinothems in three bedsets and one basal zone. The Panther Tongue contains a total of 14 surfaces representing 13 clinothems within a single bedset (Fig. 6).

Building the 3D geological grids

Once generated, the bed-based surfaces of individual clinothems were used to create modelling zones in which 3D grids were built. Zone boundaries delimit the fundamental cellular framework within RMS. In the models built, each single clinothem was represented by a separate zone. When constructing the grid, the size and number of cells and hence the horizontal and vertical resolutions are set. Ideally the grid should be orientated parallel to the main geological heterogeneity and the model-grids were aligned with the principal progradation direction of the respective delta systems (For details see Enge et al., Submitted-b; Enge et al., Submitted-a). The Panther Tongue model is 670 x 1100 x 16 m (XYZ). The Ferron model is smaller aerially but slightly thicker 500 x 500 x 25 m (XYZ) The grid cell size in both models is 10 x 10 x 0.2 m giving 337311 cells in the Panther Tongue models and 239147 in the Ferron models (Fig. 7). The grid was built “top conformable” for each zone to reflect the downlapping geometry at the base of the clinothem and the corners were collapsed.

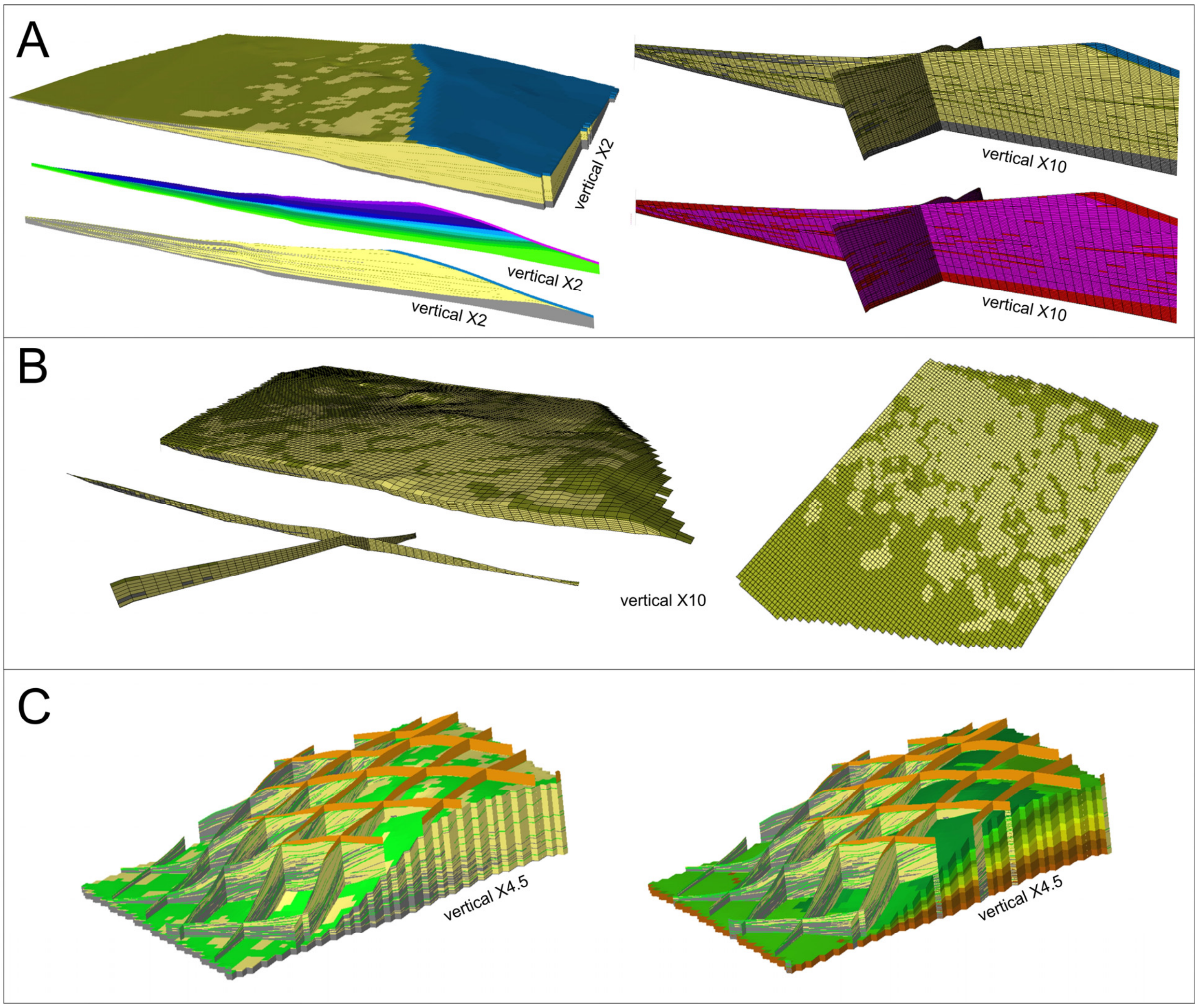

Fig. 7. The grid models populated from zones, or with facies or pethrophysical values, highlighted in different colours. **(A)** Panther model coloured by zones or facies (left), and X10 vertical exaggeration of cross sections showing facies or petrophysical values (red – low permeability; pink – higher permeability values) (right). **(B)** Single zone / clinothem populated with facies. Note holes (yellow) in barrier (green) in top layer. **(C)** Ferron model cross-section coloured from facies shown with lower part of grid model (left) and zones (right). All models: Green - siltstone; yellow - sandstone; blue - lag (Panther Tongue); orange - marginal marine (Ferron).

While both models are extremely detailed, the number of cells is low enough that the static model can be flow simulated without need for upscaling (Fig. 7). This was an important consideration in designing the grid and reduces the introduction of upscaling errors.

Assigning properties to the grid

Once built, the 3D grid was populated with properties. The first stage was to assign facies to the cells; the second stage was to assign petrophysical values to the facies.

Geological properties

The surfaces mapped and logged in the field and the VOM were recreated in the model deterministically. The facies at the outcrop could also be placed in the model deterministically but stochastic methods were required to populate the unseen parts of the volume. Five lithofacies were modelled: delta front sandstone which occurs in the proximal part of the clinothem; prodelta siltstone, which occurs in the distal part of the zone; draping siltstone, which occurs between the clinothems; the transgressive lag, a coarse sandstone that caps the Panther Tongue (Fig. 8); and marginal marine siltstones that cap the Ferron Sandstone bedsets. The transgressive lag is only present where the top of the Panther Tongue model corresponds to the top of the outcrop (Hwang and Heller, 2002), which is the case for approximately one third of the area.

The correct representation of the outcrop facies distribution was accomplished by a combination of the Gaussian-based Facies:Belts and Facies:Composite tools in RMS (see MacDonald and Aasen, 1994 for an overview of these methods; Howell et al., 2008). Although stochastically-based, manipulating these methods renders a high degree of control on the facies distribution and hence an accurate representation of the geology from the outcrop in the models.

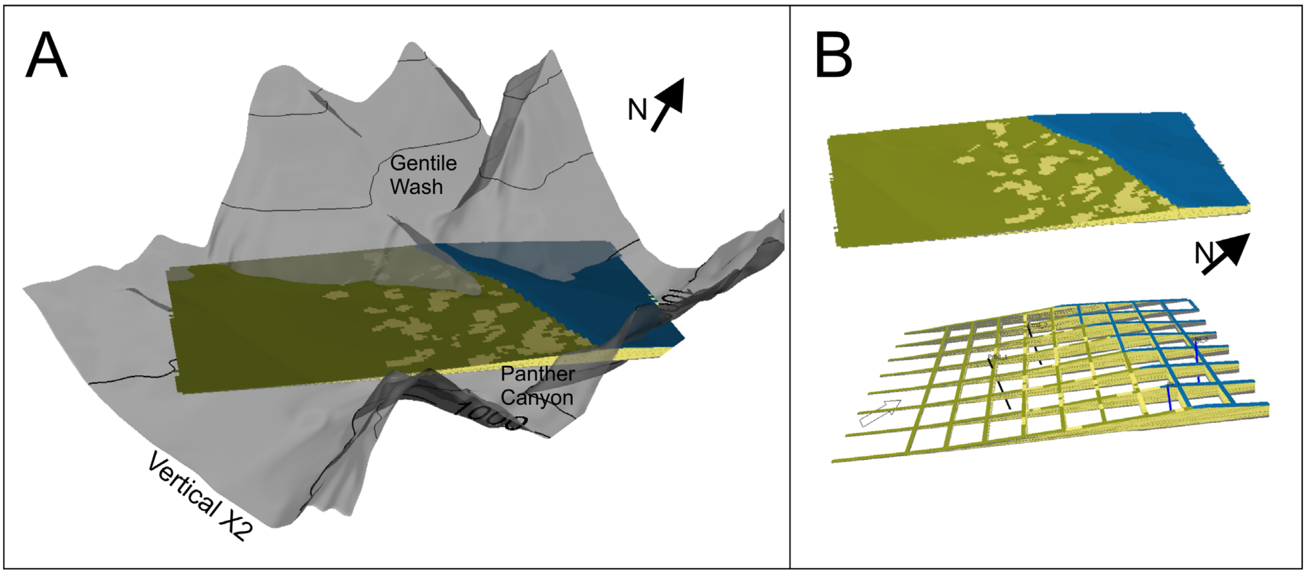

Fig. 8. Facies model of the Panther Tongue. **(A)** Model and terrain. **(B)** Model (top) and cross sections with wells (bottom).

The models were built in the following stages

1. The Facies:Belts tool was used to place delta front sandstone passing to prodelta siltstone in the body of the clinothem. The tool allows a gradational, interfingered contact to be achieved. The position of the contact is based on the outcrop observations.
2. A 20 cm layer (one grid cell thickness) of siltstone is then placed at the top of the zone to represent the draping siltstone. This is achieved using a facies parameter filter on the grid to set the first layer of the zone to the required parameter.
3. If holes are required in the draping siltstone layer, a Facies:Composite model is created in a separate version of the zone. Disk-shaped sandstone bodies (holes) are modelled in a neutral background. The proportion of sandstone bodies depends upon the required proportion of holes. The objects are created with a 1D linear trend parallel to the depositional dip direction. This results in more of the sandstone bodies "holes" occurring in an updip position and less down dip. This reflects the greater amount of siltstone that is eroded in the upper part of the delta front.
4. The two versions of the zone are merged such that the sandstone bodies replace the shale in the draped layer and thus the holes are produced.

The process is repeated for each zone until finally the transgressive lag (Panther Tongue) and the marginal marine siltstone (Ferron) are modelled deterministically. Once completed the facies models are quality controlled by visual inspection and comparison to the virtual outcrop.

Petrophysical properties

The lithofacies control the distribution of petrophysical properties. Deterministic petrophysical properties were assigned to the various facies. The sandstones were assigned a porosity of 25%, a vertical permeability (Kv) of 1.95 mD and a horizontal permeability (Kh) of 90 mD. This was constant in all of the models. The porosity of the siltstones was a constant 5% while the permeability was varied in different models from 0.001 to 1 mD (see above) with Kv equal to Kh. Stochastic procedures were not employed as these would have introduced additional noise in the results and confused the intentions of testing the impact of heterogeneities. All values chosen are typical for subsurface reservoirs (Manzocchi et al., 2008).

Experimental design

A total of 41 models were built and flow simulated. Two base-case models, one from the Ferron and one from the Panther Tongue were used to compare a highstand delta with a forced regressive delta system. The Ferron model is smaller than the Panther Tongue but contains significant more bedsets (three versus one) and steeper dipping clinoforms (2.6° versus 1.25°). Further details of the geometric differences between the two systems are presented in Enge et al (Submitted-a). Twenty children models were built of each of the two base case models. Within these the proportion of holes in the clinoform silt and the silt permeability were systematically varied as discussed above (Table 1 and Fig. 5).

Flow simulation

Two phase flow simulation was considered to the best method for dynamically investigating and comparing the effects of the heterogeneities on reservoir performance. Previous modelling studies from the areas include Ainsworth et al. (1999), who used the Panther Tongue as a template for modelling a producing subsurface oil field, but did not extract quantitative data from the outcrops. Several authors have performed analogue reservoir modelling from the river-dominated parts of the Ferron Sandstone (e.g. Froster et al., 2004; van den Bergh and Garrison, 2004) who used a regular grid conditioned with outcrop data.

Flow simulation was performed using the RMS finite difference black oil simulator. The properties used to condition the models are summarized in table 2. As the purpose was to test the effect of holes and varying permeability values in siltstone layers, all other properties were kept constant in all model runs. The flow simulations were based upon two through-going vertical water injection wells and two vertical production wells. In the Ferron model the production wells were placed in a line in the thicker updip position and the injectors in a line down dip, closer to the clinothems toes, resulting in an updip flow. The two injectors and the two producers were 150 m apart, and the injectors and producers were 250 m apart. This approximates to 20 acre development spacing. The Panther Tongue area has been subjected to tectonic tilting and due to the desire to generate flow upwards, the setup was opposite that of Ferron. Two injector wells were placed in the thicker updip position and two producer wells in the thinner downdip position. The two production wells and the two injector wells were 250m apart, respectively, and the production and injector wells were placed 550 m apart. Note that the smaller Ferron model had the wells in a single injector and producer pair placed closer than the larger Panther Tongue model.

Flow rates of 500 Sm3/day were used for both injectors and producers, and a fixed bottom-hole pressure of 300 bars was set for the injectors (Table 2). Simulations were run until one pore volume of water was injected, theoretically corresponding to a flushing of water through all pores. For the Panther Tongue model this corresponded to approximately 900-1000 days, for the Ferron roughly 400-450 days. The numbers vary due to different pore volumes in the different models. All models experienced water breakthrough within the time of simulation.

The purpose of this exercise was to use flow simulation as a dynamic test of reservoir response to the presence of heterogeneities and generate values for comparison between various models. More sophisticated simulation approaches and optimization of the production are beyond the scope of this study.

A total of 41 (20 + 21) models were flow simulated and simulation results were used to address the following questions:

1. How do different numbers of holes and permeability values for the siltstone affect simulated fluid flow; and what is more important with regards to recovery; holes or silt permeability?
2. Does the higher frequency of heterogeneities related to the steeper and shorter clinothems in the Ferron Sandstone produce differently than the Panther Tongue with lower frequency of heterogeneities related to longer and less steep clinothems?
3. What effect does well placing have on simulated production in the two systems?

Four key production parameters were monitored and are considered in the following: oil saturation, production rate field, total production field, and recovery factor.

Table 2. Flow simulation dynamic properties.

Length of runs	Until injection of one pore volume. Panther Tongue: 888 –1071 days Ferron Sandstone: 408 – 544 days
Report step	One quarter
Rock compressibility	0.0000435 /bar
Rock reference pressure	275.79 bar
Spec. gravity oil	0.8
Gas / oil ratio	142.486 Sm3/Sm3
Corey exp	Water 4 Oil – water 3
Saturation end points	Sorw: 0.2 Swct 0.2
Rel. perm. end points	Kromax 1 Krw 0.4
Oil Water Contact	1015 m (below model)
OWC capillary pressure	0
Reference depth	1030 m
Reference pressure	103 bar
Flow rate wells	Injector (2): 500 Sm3 / day Producer (2): 500 Sm3 / day
Bottom hole pressure	Injectors: 300 bar
Initial oil in place	*Ferron Sandstone:* 0 % holes: 337377 rm3 30 % holes: 360902 rm3 30 % holes, extra barrier: 360902 rm3 60 % holes: 382337 rm3 90 % holes: 420780 rm3 100 % holes: 440520 rm3 *Panther Tongue:* 0 % holes: 706019 rm3 30 % holes: 750376 rm3 60 % holes: 794508 rm3 90 % holes: 833658 rm3 100 % holes: 845743 rm3

Results

The simulation results from the two sets of model show systematic variations and key differences. The results are summarized in table 3 and figures 9-11. In both suites of models the proportion of holes and the siltstone permeability values both influence the production, but differently for the two suites. The portion of holes governs the production rate and hence the recovery factor in the Panther Tongue models, whereas permeability values are more important in the Ferron models, although it is still influenced by the number of holes. Also, until water breakthrough, for any given hole model, the higher permeability models always produced better than the lower permeability ones, indicating that shale permeability is the more important of the two factors.

The models from the Panther Tongue and the Ferron Sandstone have different initial in place volumes (Table 2), therefore, the models are best compared by considering the recovery factor (in place oil/produced volume) The Panther Tongue models show a modest spread in recovery factor from 41.1 to 46.4%, apparently controlled by the proportion of holes (Fig. 9B). The Ferron models show a much broader range of recoveries between 13.8 and 43.1%, much appear to be more dependent upon the permeability of the siltstone layers (Fig. 9A).

Both models experienced an initially high production rate, which steadily declined through time and then suddenly dropped as the injected water reached the production well (water breakthrough). Compared to Ferron, the Panther Tongue models maintains a relatively high production rate for over a year of production, whereas reduction in production rate declines much faster in the Ferron models.

In the Panther Tongue models, the production rate for the different hole models are lowest for the models with the least holes and increase successively to the model with no siltstone drapes (Fig. 10). This pattern is maintained until water cut after approximately a year of production. After water break though production rates drop from a rate of 500 to 700 Sm3 to about 100 Sm3 a day within 200 days. The production rate of the model with no siltstone drapes drops significantly faster than any other model and changes over a time span of 100 days from having the highest production rate to producing at the rate of the worst models. Conversely the drop in production rates after water breakthrough is less marked in the tightest models.

Table 3. Summary of flow simulation results.

	Model code *(%holes_KvKhSiltStone)*	**Total production (Sm3)**	**Recovery Factor (%)**	**Length of run (days)**
Ferron Sandstone Models	00_1mD	124325	36.9	366
	00_0_1mD	112693	33.4	366
	00_0_01mD	75402	22.3	366
	00_0_001mD	46585	13.8	366
	30_1mD	134164	37.2	366
	30_0_1mD	123131	34.1	366
	30_0_01mD	89826	24.9	366
	30_0_001mD	65437	18.1	366
	60_1mD	152575	39.9	456
	60_0_1mD	143189	37.5	456
	60_0_01mD	119289	31.2	456
	60_0_001mD	93595	24.5	456
	90_1mD	176849	42	456
	90_0_1mD	169643	40.3	456
	90_0_01mD	158274	37.6	456
	90_0_001mD	147031	34.9	456
	100_1mD	189939	43.1	456
	100_0_1mD	183815	41.7	456
	100_0_01mD	175188	39.8	456
	100_0_001mD	167790	38.1	456
	30_0_1mD_*ExtraBarrier*	133527	37.0	366
Panther Tongue Models	00_1mD	311113	44.1	821
	00_0_1mD	305147	43.2	821
	00_0_01mD	298380	42.3	821
	00_0_001mD	290313	41.1	821
	30_1mD	339145	45.2	912
	30_0_1mD	333786	44.5	912
	30_0_01mD	328625	43.8	912
	30_0_001mD	323897	43.2	912
	60_1mD	364019	45.8	1004
	60_0_1mD	359231	45.2	1004
	60_0_01mD	355030	44.7	1004
	60_0_001mD	351711	44.3	1004
	90_1mD	381523	45.8	1004
	90_0_1mD	377044	45.2	1004
	90_0_01mD	373680	44.8	1004
	90_0_001mD	371246	44.5	1004
	100_1mD	392733	46.4	1004
	100_0_1mD	388499	45.9	1004
	100_0_01mD	385534	45.6	1004
	100_0_001mD	383618	45.4	1004

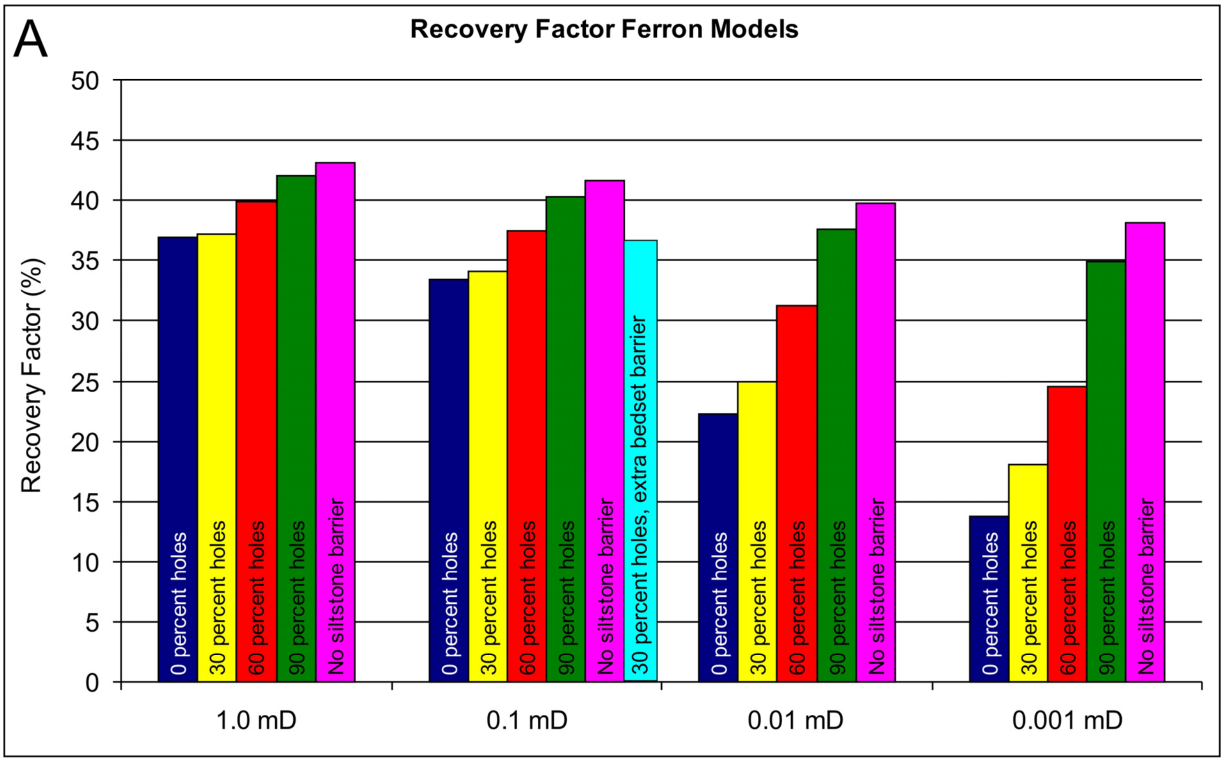

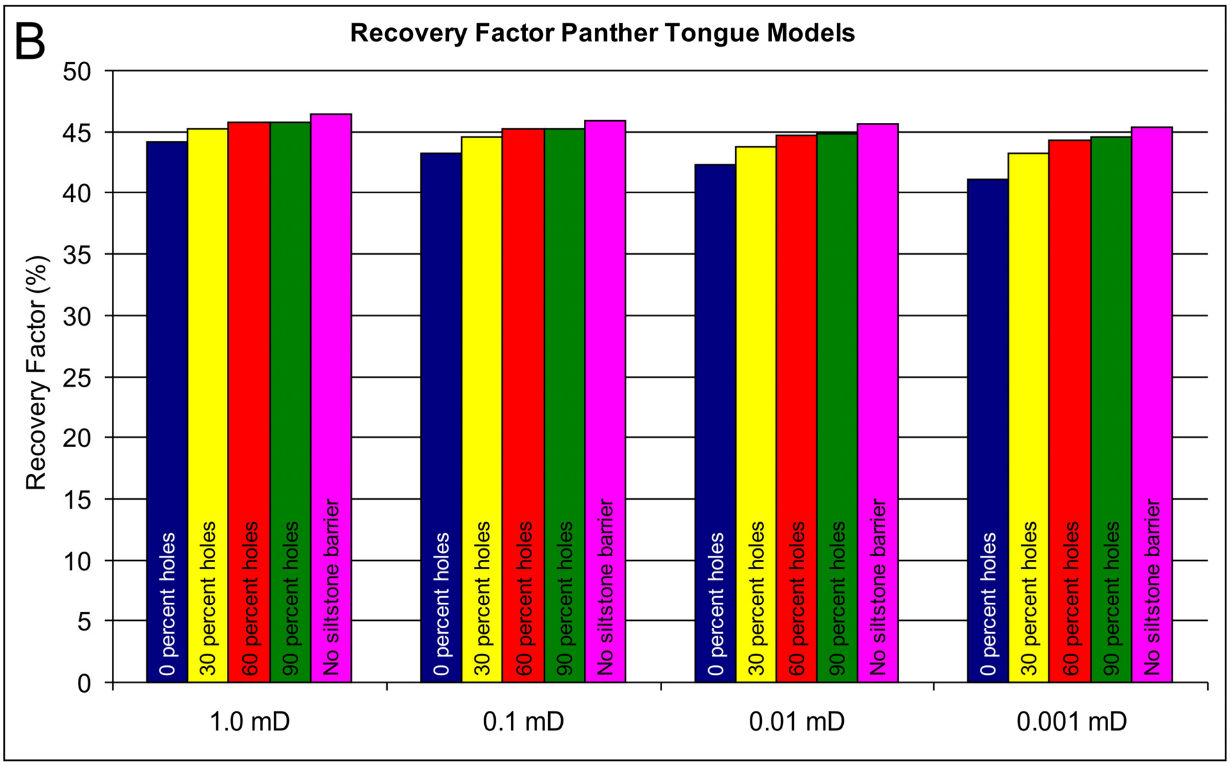

Fig. 9. Recovery factor results from flow modelling. **(A)** Ferron Sandstone models. **(B)** Panther Tongue models. Note variations in the Ferron results compared to the Panther Tongue results.

The recovery factor show some overlap between the different hole models, with the models with the highest siltstone permeabilities (Kv/Kh = 1mD) and holes of the three (30, 60 and 90%) producing better than the two tightest (Kv/Kh = 0.01 and 0.001 mD) model with no siltstone drapes. Also, the spread in the recovery factor is highest for the tightest no hole models, from 41.1 to 44.1%, and lowest in the all hole model, from 45.5 to 46.4%.

In spite of the fact that 80% of the lithology in the studied Ferron Sandstone interval is sandstone (Mattson and Chan, 2004), in the Ferron models, the production rate is heavily influenced by the siltstone permeability values (Fig. 11). Over the time period from the start of the simulation to water breakthrough after about 100 days, the production rate for the different hole models shows a wide spread depending on the siltstone permeability. The models with fewer holes have lower production rates until water breakthrough. These few-holes models experience some stabilization in production rates after water breakthrough. The open model produces with the highest rates, but the relative difference is higher between the models with the different permeability values. After water breakthrough, as water production increases, oil production rate decreases for all models over the next 200 days, before ending end up at around 100 Sm3 a day.

In the Ferron model the recovery factor for the models without holes varies between 13.8 to 36.9%. The spread is much smaller (38.1 to 43.1 %) in the model with no siltstone barriers. There is a high degree of overlap between the different models depending on the permeability values. This is especially the case for all models with permeability set to 1.0 or 0.1 mD, although the more holes in the models, the less spread of the values.

The role of dipping clinothem heterogeneities

The models from both the Panther Tongue and the Ferron Sandstones are clearly influenced by the presence of silt draped clinoforms. Holes in the shale drapes and variations in the siltstone permeability control production. In the Panther models, tighter siltstone layers do not result in overlapping results from different hole models, whereas this is the case for the Ferron models (Figs. 10 and 11).

The area modelled from the Ferron is much smaller than that of the Panther Tongue model. The Ferron however has much more closely-spaced clinothems and hence barrier layers. The great spread in cumulative production and recovery for the tightest Ferron models indicate

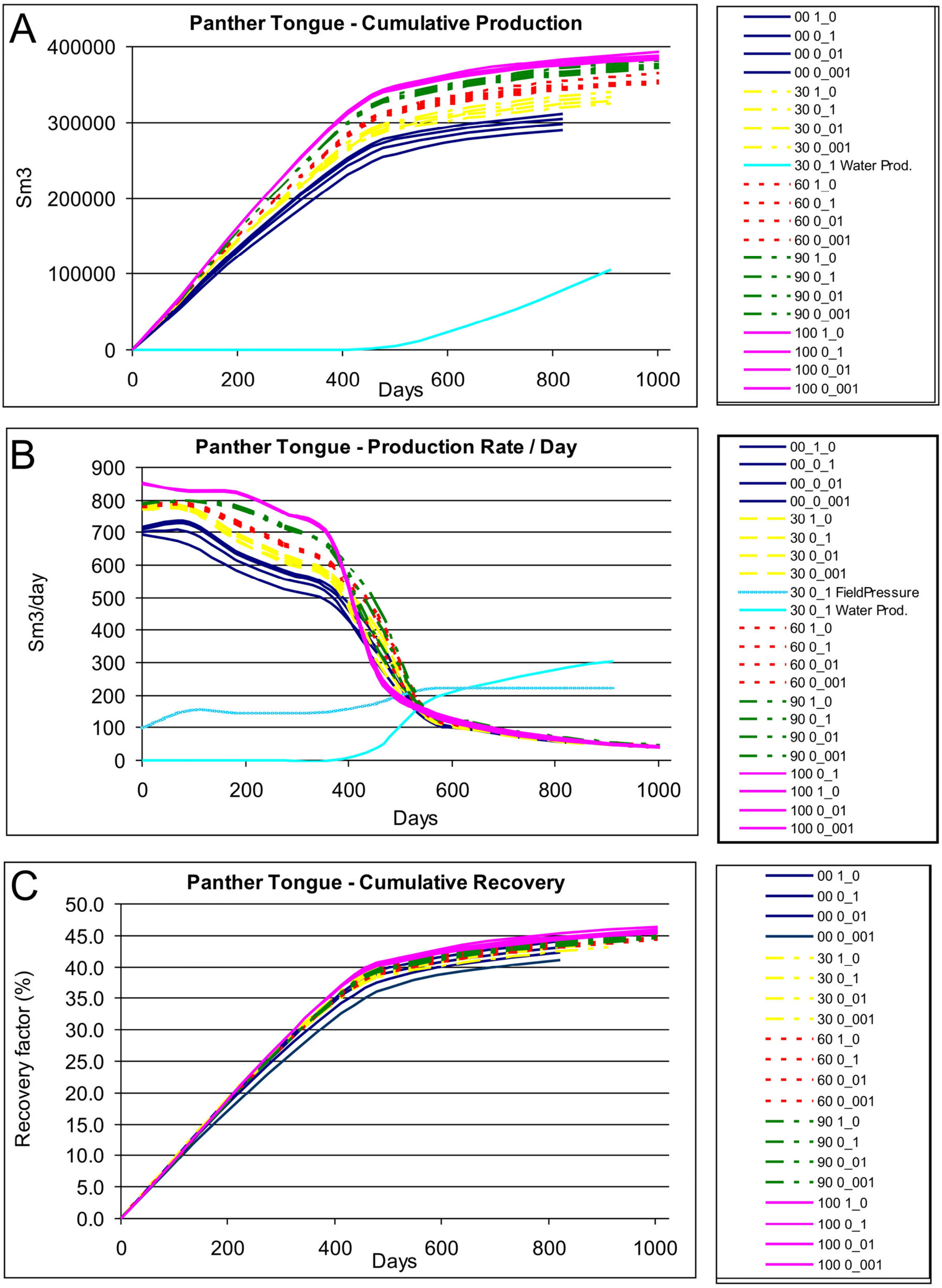

Fig. 10. Flow simulation results from the Panther Tongue models. Simulations were run until one pore volume of water was injected. In addition to oil production results, field pressure and water production for the 30 %, 0.1 mD run are plotted. **(A)** Cumulative production. **(B)** Production rate per day. **(C)** Cumulative recovery.

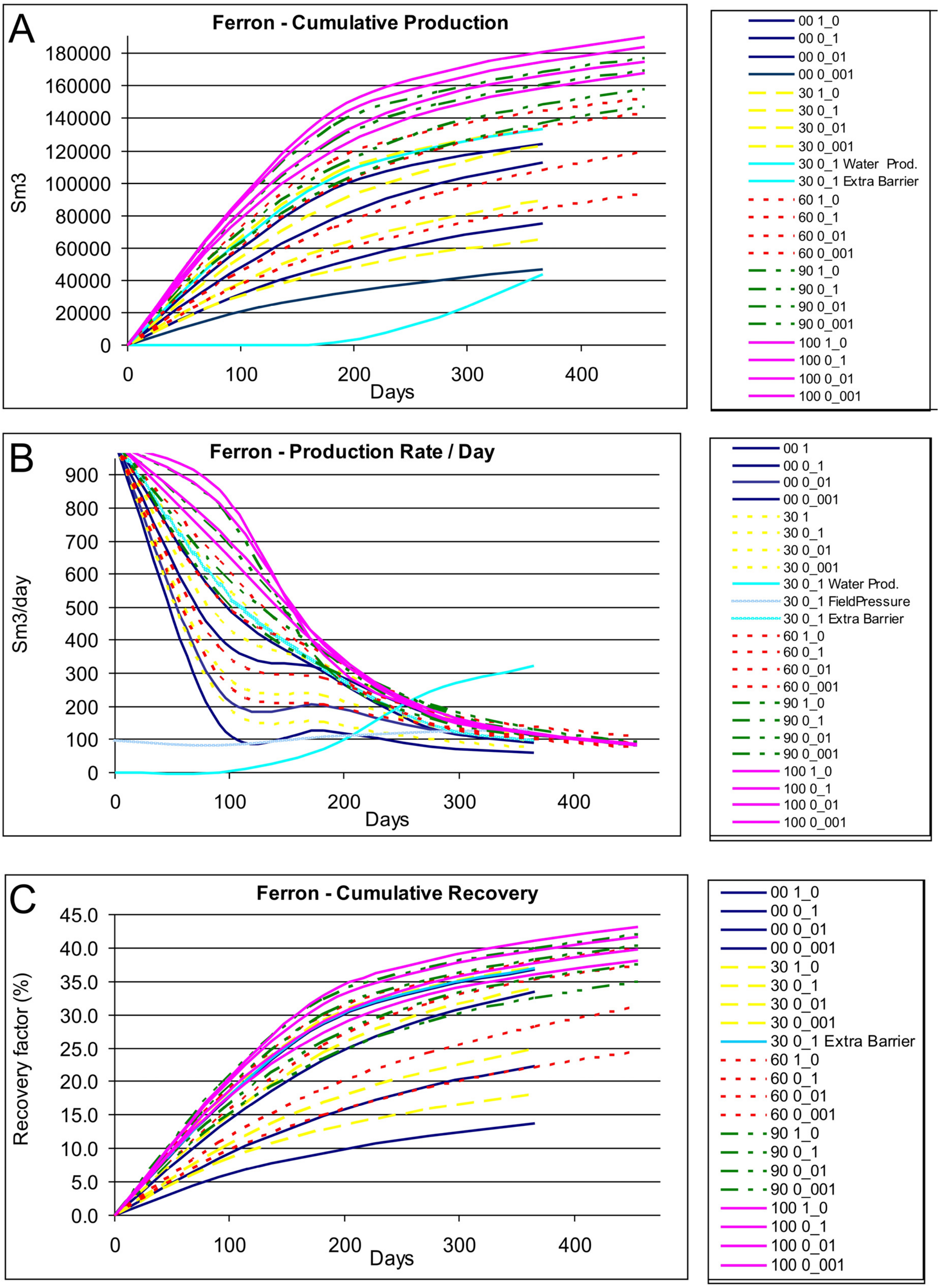

Fig. 11. Flow simulation results from the Ferron models. Simulations were run until one pore volume of water was injected. In addition to oil production results, field pressure and water production for the 30%, 0.1 mD-run are plotted. **(A)** Cumulative production. **(B)** Production rate per day. **(C)** Cumulative recovery.

that permeability is the key factor governing the production in the three tightest models, resulting in a torturous flow path leading to lower production. Such effects were also noted by Skorstad et al. (2008) when modelling synthetic shallow-marine reservoirs. Production in the Panther Tongue model is dominated by low angle clinothems which extend between the wells while the shorter and steeper clinothems in the Ferron model do not (Enge et al., Submitted-b; Enge et al., Submitted-a) (Fig. 6)**.** This implies that both produced oil and injected water is forced to either pass around barriers or go through it.

The best recovery is obtained with the combination of high permeability and few or no barriers, as illustrated in figure 12 from two Ferron models, comparing different time steps of the 30% holes and 0.1 mD models with the 0% holes and 1 mD model. Whereas the first experienced a smooth production path and injected water spreads out evenly, the latter encounters both low production and slow diffusion of injected water. Clearly, these deviating patterns are controlled by the higher amount of barriers and also low permeability values in the tighter model compared to the mid range model, resulting in a recovery of 13.8 and 34.1%, respectively.

In any models from the Ferron, only when permeability is 0.1 mD or above does the recovery significantly exceed 30%. The influence of the holes are most important only when there are 90% or more of them, i.e. almost no barriers, or the permeability in the siltstone layers are 0.1 mD or better. However, the overall results are significantly better for the models with the most holes compared to the ones with fewer. This indicates that the holes represent conductors to flow through the barrier layers, still allowing for some production in otherwise tight models.

Unexpectedly, tighter barriers also enhanced recovery. In otherwise equal models, three bedset boundaries of the 30 % hole and 0.1 mD permeability model from Ferron were equipped with two cells thickness barrier (2 x 0.2 m, twice the normal). This shifted the recovery results *up* almost to the level of the ordinary 1.0 mD-model, and significantly above the ordinary 0.1mD model (Fig. 11). A possible explanation to this is that the flow was lead to the holes more efficiently, and in this way reduced the travel time to the producer. A lengthened flow path of the injected water can lead to increased sweep when modelling clinothems, as discussed by Jackson et al. (2005).

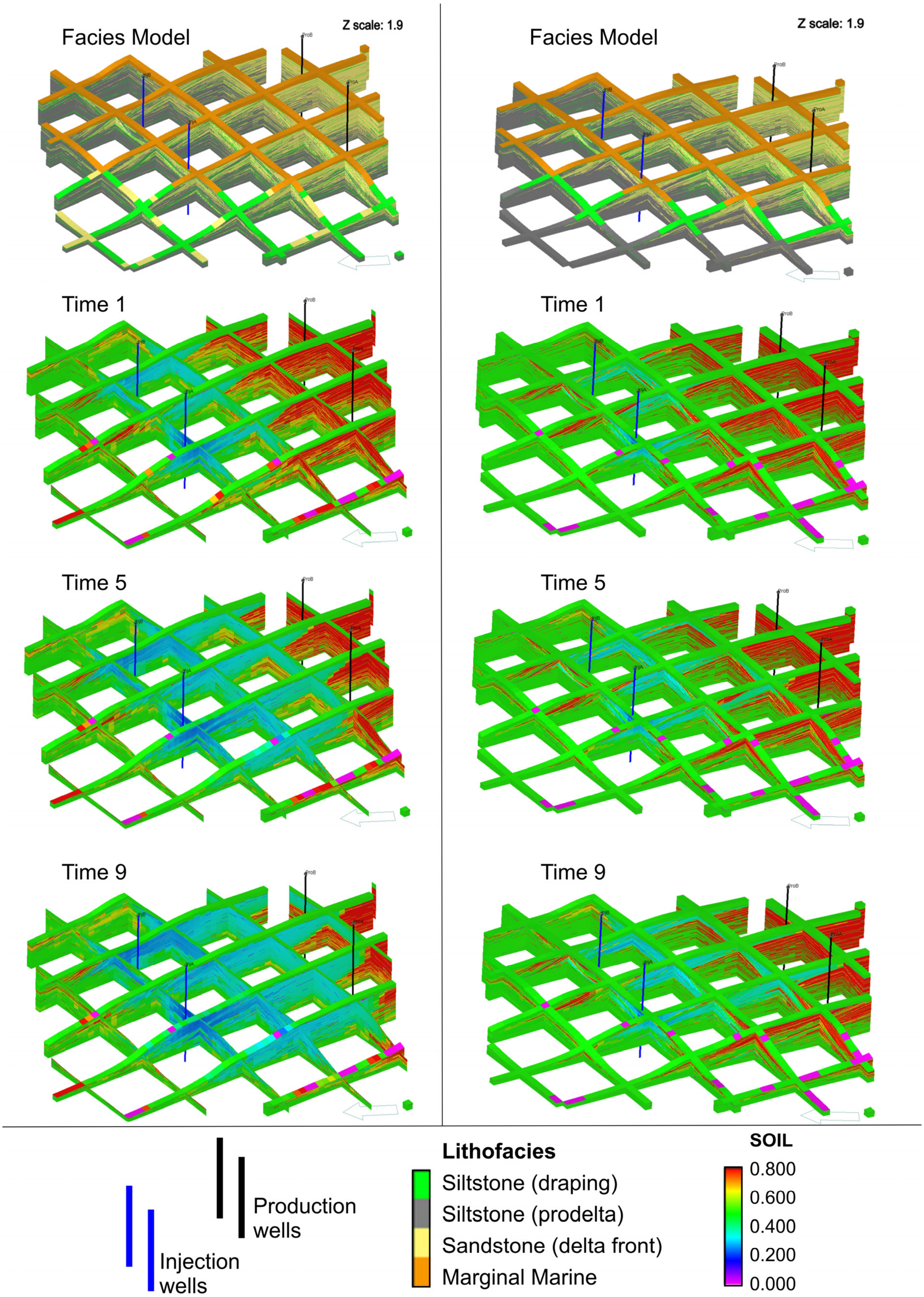

Fig. 12. Flow simulation comparison between time steps from Ferron model 30 % holes / 0.1mD **(left)** and Ferron model 0 % / 1mD **(right)**. SOIL= Oil Saturation. Note lower sweep efficiency in right hand models.

Discussion

In common with other river-dominated deltaic systems, the sandstone clinothem beds and bedsets of the Panther Tongue and the Ferron Sandstone are interbedded with siltstone beds and lamina (Ainsworth et al., 1999; Howell et al., 2008; Howell et al., in press). These siltstones are expected to produce dipping barriers and baffles to hydrocarbon fluid flow (Ainsworth et al., 1999; Froster et al., 2004; Howell et al., 2008; Skorstad et al., 2008; Howell et al., in press), although none of these studies perform flow simulation test at the scale of individual clinothems.

The present study demonstrates that clinothem and associated heterogeneities have significant influence on production. Explicitly modelled, manipulating the properties of the siltstone associated with the clinoforms alter recovery factors by as much as 25% in otherwise equal models. When present as elements which do not extend between wells, as is mostly the case in the Ferron models, they have a greater influence on production than when represented as field-wide reservoir elements, as in the Panther Tongue model. As a result of this, not only do the Ferron models on average have worse production than the Panther Tongue models, they also experience a higher degree of reservoir compartmentalisation.

The length:width ratio of clinothems described by Enge et al. (Submitted-a), is a guide for optima placement of wells, which is illustrated by the present study. The spacing of wells also has to be considered against the possibility of early water breakthrough in the producer well. Too early water cut lowers the oil sweep and hence recovery. The longer and more continuous clinothems of the falling to lowstand system tract deposits of the Panther Tongue requires a vertical well spacing of injectors and producers of less than 700 m, and most likely as close as 500 m (this study). By wider spacing there is an increased risk of injecting into and producing from clinothems of different mouth bar complexes, with from low to no connections depending on permeability values, and hence risking compartmentalisation of the reservoir.

In high-stand system tracts like the Ferron Sandstone, present results indicate that well placing should ideally be guided by recorded permeability values. The lower the permeability values, the closer the wells have to be spaced not to risk too high a degree of reservoir compartmentalisation. Even with spacing of vertical injector and producer wells as close as 250 m (this study), barriers related to heterogeneities have significant influence on production. Wider spacing of wells will be influenced both by bed and bedset heterogeneities.

Although some of the results in this study might indicate otherwise, over the time span of a producing field the latter is expected to act as a significant barrier to flow. This is due to the expected thicker siltstone and less likelihood of holes, in addition to represent a risk of juxtaposition due to lobe switching, as the bedset boundaries represent a longer time span than the bed boundaries.

Conclusions

The present study demonstrates the influence of clinothem related heterogeneities on simulated hydrocarbon production. A suite of analogue reservoir models were built from the Ferron Sandstone and the Panther Tongue. The former represent a highstand system tract system whereas the latter is interpreted as falling to lowstand system tract deposits.

The results indicate that steeper dipping and closer spaced clinothems of the highstand system tract lower the recovery factor by several tens of percent if the related heterogeneities are close to continuous and have low enough permeability. A consequence of this is low sweep efficiency and reservoir compartmentalisation. The results indicate that spacing of injector and producer wells in a subsurface reservoir ideally should be guided by the actual condition of the clinothem spacing and related permeability.

The present study also proves the value of laser scanning as a tool for both building virtual outcrops for quantitative reservoir characterisation as well as to be used as input for reservoir modelling.

Acknowledgments

Simon Buckley and Christian Carlsson are thanked for assistance and tireless effortless in the field, and Henning Nøttveit and Jan Tveranger for technical help in the reservoir modelling process. The Norwegian Research Council provided financial support together with equipment contributions from StatoilHydro ASA through the Petromaks programme (project 163264). Riegl Laser Measurement Systems GmbH is acknowledged for providing software support and Roxar generously provided the Irap Roxar RMS-software.

.

References

Ainsworth, R.B., Sanlung, M. and Duivenvoorden, S.T.C. (1999) Correlation technique, perforation strategies, and recovery factors; an integrated 3-D reservoir modeling study, Sirikit Field, Thailand. *AAPG Bulletin*, **83,** 1535-1551

Anderson, P.B., Chidsey, T.C., Ryer, T.A., Adams, R.D. and McClure, K. (2004) Geologic framework, facies, paleogeography, and reservoir analogs of the Ferron Sandstone in the Ivie Creek area, east-central Utah. In: *Regional to wellbore analog for fluvial-deltaic reservoir modeling; the Ferron Sandstone of Utah* (Eds T.C. Chidsey, R.D. Adams and T.H. Morris), *American Association of Petroleum Geologists Studies in Geology 50*, pp. 331-356. American Association of Petroleum Geologists, Tulsa, Oklahoma, United States.

Anderson, P.B. and Ryer, T.A. (2004) Regional Stratigraphy of the Ferron Sandstone. In: *Regional to Wellbore Analog for Fluvial-Deltaic Reservoir Modeling: The Ferron Sandstone of Utah* (Eds T.C. Chidsey, R.D. Adams and T.H. Morris), *AAPG Studies in Geology 50*, pp. 211-224. American Assocaition of Petroleum Geologists, Tulsa, Oklahoma, USA.

Bhattacharya, J.P. and Davies, R.K. (2001) Growth faults at the prodelta to delta-front transition, Cretaceous Ferron Sandstone, Utah. *Marine and Petroleum Geology*, **18,** 525-534

Bhattacharya, J.P. and Walker, R.G. (1992) Deltas. In: *Facies Models: Response to Sea Level Change* (Eds R.G. Walker and N.P. James), pp. 157-177. Geological Association of Canada, St. John's, Canada.

Bhattacharya, J.P. and Willis, B.J. (2001) Lowstand deltas in the Frontier Formation, Powder River basin, Wyoming: Implications for sequence stratigraphic models. *AAPG Bulletin*, **85,** 261-294

Bryant, I.D. and Flint, S.S. (1993) Quantitative clastic reservoir geological modelling; Problems and perspectives. In: *The geological modelling of hydrocarbon reservoirs and outcrop analogues* (Ed I.D. Bryant), **15**, pp. 3-20. Blackwell, Oxford, International.

Buckley, S.J., Howell, J.A., Enge, H.D. and Kurz, T.H. (2008) Terrestrial laser scanning in geology: data acquisition, processing and accuracy considerations. *Journal of the Geological Society of London*, **165,** 625-638

Buckley, S.J., Howell, J.A., Enge, H.D., Leren, B.L.S. and Kurz, T.H. (2006) Integration of terrestrial laser scanning, digital photogrammetry and geostatistical methods for high-resolution modelling of geological outcrops. In: *ISPRS Commission V Symposium September 25-27*, *International Archives of the Photogrammetry, Remote Sensing and Spatial Information Sciences*, **36(B5)**. Commission V, WG III. http://rcswww.urz.tu-dresden.de/~isprs/proceedings/paper/1228_Dresden06.pdf, Dresden, Germany.

Catuneanu, O. (2006) *Principles of Sequence Stratigraphy*. Elsevier, Amsterdam, 375 pp.

Cross, T.A. (1986) Tectonic controls of foreland basin subsidence and Laramide style deformation, Western United States. In: *Foreland basins*, **8**, pp. 15-39. Blackwell, Oxford, International.

Dreyer, T., Falt, L., Høy, T., Knarud, R., Steel, R. and Cuevas, J.-L. (1993) Sedimentary architecture of field analogues for reservoir information (SAFARI): A case study of the fluvial Escanilla Formation, Spanish Pyrenees. In: *The Geological modelling of hydrocarbon reservoirs and outcrop analogues* (Eds S.S. Flint and I.D. Bryant), *London, International Association of Sedimentologists Special Publication*, **15**, pp. 57-79. Blackwell.

Enge, H.D., Buckley, S.J., Rotevatn, A. and Howell, J.A. (2007) From outcrop to reservoir simulation model: workflow and procedures. *Geosphere*, **3,** 469-490

Enge, H.D., Howell, J.A. and Buckley, S. (Submitted-a) Contrasting bedsets in river dominated deltas: examples from the Panther Tongue Member and the Ferron Sandstone Member, Utah, USA. *Journal of Sedimentary Research*

Enge, H.D., Howell, J.A. and Buckley, S. (Submitted-b) Quantifying clinothem geometry in a forced-regressive river-dominated delta, Panther Tongue, Utah, USA. *Sedimentology*

Fouch, T.D., Lawton, T.F., Nichols, D.J., Cashion, W.B. and Cobban, W.A. (1983) Patterns and timing of synorogenic sedimentation in Upper Cretaceous rocks of central and Northeast Utah. In: *Mesozoic paleogeography of the West-Central United States*, **2**, pp. 305-336. Society of Economic Paleontologists and Mineralogists Rocky Mountain Section, Denver, CO, United States.

Froster, C.B., Snelgrove, S.H. and Koebbe, J.V. (2004) Modelling permeability structureand simulating fluid flow in a reservoir analog: Ferron Sandstone, Ivie Creek Area, East-Central Utah. In: *Regional to wellbore analog for fluvial-deltaic reservoir modeling:Ferron Sandstone of Utah* (Eds T.C. Chidsey, R.D. Adams and T.H. Morris), *Tulsa, Oklahoma, American Association of Petroleum Geologists, Studies in Geology*, **50**, pp. 359-382.

Gani, M.R. and Bhattacharya, J.P. (2005) Lithostratigraphy versus chronostratigraphy in facies correlations of Quaternary deltas: Application of bedding correlation. In: *River deltas; concepts, models, and examples*, **83**, pp. 31-48. Tulsa, Oklahoma, USA, SEPM (Society for Sedimentary Geology).

Gardner, M.H., Cross, T.A. and Levorsen, M. (2004) Stacking patterns, sediment volume partitioning, and facies differentiation in shallow-marine and coastal-plain strata of the Cretaceous Ferron Sandstone, Utah. In: *Regional to wellbore analog for fluvial-deltaic reservoir modeling; the Ferron Sandstone of Utah*, **50**, pp. 95-124. American Association of Petroleum Geologists, Tulsa, OK, United States.

Garrison, J.R. and van den Bergh, T.C.V. (2004) High-resolution depositional sequence stratigraphy of the upper Ferron Sandstone Last Chance Delta; an application of coal-zone stratigraphy. In: *Regional to wellbore analog for fluvial-deltaic reservoir modeling; the Ferron Sandstone of Utah*, **50**, pp. 125-192. American Association of Petroleum Geologists, Tulsa, OK, United States.

Howard, J.D. (1966) *Upper Cretaceous Panther Sandstone Tongue of East-Central Utah, Its Sedimentary Facies and Depositional Environments*, Brigham Young University, Provo, 155 pp.

Howell, J.A., Skorstad, A., MacDonald, A., Fordham, A., Flint, S., Fjellvoll, B. and Manzocchi, T. (2008) Sedimentological parameterization of shallow-marine reservoirs. *Petroleum Geoscience*, **14,** 17-34

Howell, J.A., Vassel, Å. and Aune, T. (in press) Modelling of dipping clinoform barriers within deltaic outcrop analogues from the Cretaceous Wesetrn Interior Basin USA. In: *The Future of Hydrocarbon modelling*, *The Geological Society of London, Special Publications*. The Geological Society of London, London, UK.

Hwang, I.-G. and Heller, P.L. (2002) Anatomy of a transgressive lag: Panther Tongue Sandstone,Star Point Formation, central Utah. *Sedimentology*, **49,** 977-999

Jackson, M.D., Yoshida, S., Muggeridge, A.H. and Johnson, H.D. (2005) Three-dimensional reservoir characterization and flow simulation of heterolithic tidal sandstones. *AAPG Bulletin*, **89,** 507-528

Jervey, M.T. (1988) Quantitative geological modeling of siliciclastic rock sequences and their seismic expression. In: *Sea-level changes; an integrated approach*, **42**, pp. 47-69. SEPM (Society for Sedimentary Geology), Tulsa, OK, United States.

Jordan, T.E. (1981) Thrust loads and foreland basin evolution, Cretaceous, western United States. *AAPG Bulletin*, **65,** 2506-2520

Kauffman, E.G. (1984) Paleobiogeography and evolutionary response dynamic in the Cretaceous Western Interior seaway of North America. In: *Jurassic-Cretaceous biochronology and biogeography of North America*, **27**, pp. 273-306. Geological Association of Canada, Toronto, ON, Canada.

Kjonsvik, D., Doyle, J., Jacobsen, T. and Jones, A. (1994) The effects of sedimentary heterogeneities on production from a shallow marine reservoir; what really matters? In: *Proceedings; European petroleum conference; Volume 1*.

Labourdette, R., Casas, J. and Imbert, P. (2008) 3D Sedimentological Modelling of a Miocene Deltaic Reservoir Unit, Sincor Field, Venezuela: A New Approach. *Journal of Petroleum Geology*, **31,** 135-152

MacDonald, A.C. and Aasen, J.O. (1994) A prototype procedure for stochastic modeling of facies tract distribution in shoreface reservoirs. In: *Stochastic modeling and geostatistics; principles, methods, and case studies*, **3**, pp. 91-108. American Association of Petroleum Geologists, Tulsa, OK, United States.

Manzocchi, T., Heath, A.E., Palananthakumar, B., Childs, C. and Walsh, J.J. (2008) Faults in conventional flow simulation models: a consideration of representational assumptions and geological uncertainties. *Petroleum Geoscience*, **14,** 91-110

Mattson, A. and Chan, M.A. (2004) Facies and permeability relationships for wave-modified and fluvial-dominated deposits of the Cretaceous Ferron Sandstone, central Utah. In: *Regional to wellbore analog for fluvial-deltaic reservoir modeling; the Ferron Sandstone of Utah*, **50**, pp. 251-275. American Association of Petroleum Geologists, Tulsa, OK, United States.

Newman, K.F. and Chan, M.A. (1991) Depositional facies and sequences in the Upper Cretaceous Panther Tongue Member of the Star Point Formation, Wasatch Plateau, Utah. In: *Geology of east-central Utah*, **19**, pp. 65-75. Utah Geological Association, Salt Lake City, UT, United States.

Olariu, C. and Bhattacharya, J.P. (2006) Terminal distributary channels and delta front architecture of river-dominated delta systems. *Journal of Sedimentary Research*, **76,** 212-233

Olariu, C., Bhattacharya, J.P., Xu, X., Aiken, C.L., Zeng, X. and McMechan, G.A. (2005) Integrated study of ancient delta-front deposits, using outcrop ground-penetrating radar, and three-dimensional photorealistic data: Cretaceous Panther Tongue Sandstone, Utah, USA. In: *River Deltas — Concepts, models, and examples* (Eds L. Giosan and J.P. Bhattacharya), *Tulsa, Oklahoma, SEPM (Society for Sedimentary Geology)*, **83**, pp. 155-177.

Pirmez, C., Pratson, L.F. and Steckler, M.S. (1998) Clinoform development by advection-diffusion of suspended sediment; modeling and comparison to natural systems. *Journal of Geophysical Research, B, Solid Earth and Planets*, **103,** 24,141-24,157

Posamentier, H.W., Jervey, M.T. and Vail, P.R. (1988) Eustatic controls on clastic deposition; I, Conceptual framework. In: *Sea-level changes; an integrated approach*, **42**, pp. 109-124. SEPM (Society for Sedimentary Geology), Tulsa, OK, United States.

Posamentier, H.W. and Morris, W.R. (2000) Aspects of the stratal architecture of forced regressive deposits. In: *Sedimentary responses to forced regressions*, **172**, pp. 19-46. Geological Society of London, London, United Kingdom.

Postma, G. (1990) Depositional architecture and facies of river and fan deltas; a synthesis. In: *Coarse-grained deltas*, **10**, pp. 13-27. Blackwell, Oxford, International.

Pringle, J.K., Howell, J.A., Hodgetts, D., Westerman, A.R. and Hodgson, D.M. (2006) Virtual outcrop models of petroleum reservoir analogues: A review of the current state-of-the-art. *First Break*, **24,** 33-42

Redfern, J., Hodgetts, D. and Fabuel-Perez, I. (2007) Digital analysis brings renaissance for petroleum geology outcrop studies in North Africa. *First Break*, **25,** 81-87

Rich, J.L. (1951) Three critical environments of deposition, and criteria for recognition of rocks deposited in each of them. *Geological Society of America Bulletin*, **62,** 1-19

Rotevatn, A., Buckley, S., Howell, J.A. and Fossen, H. (in press) Overlapping faults and their effect on fluid flow in reservoirs of different depositional origin: using LIDAR data in outcrop modeling of structural complex reservoir analogues. *AAPG Bulletin*

Rotevatn, A., Fossen, H., Hesthammer, J., Aas, T.E. and Howell, J.A. (2007) Are relay ramps conduits for fluid flow? Structural analysis of a relay ramp in Arches National Park, Utah. In: *Fractured reservoirs*, **270**, pp. 55-71. Geological Society of London, London, United Kingdom.

Roxar (2008) *User guide interactive reservoir analysis package (IRAP) RMS 9.0*. Roxar Software Solutions, 2335 pp.

Ryer, T.A. (1981) Deltaic coals of Ferron Sandstone Member of Mancos Shale; predictive model for Cretaceous coal-bearing strata of Western Interior. *AAPG Bulletin*, **65,** 2323-2340

Ryer, T.A. and Anderson, P.B. (2004) Facies of the Ferron Sandstone, east-central Utah. In: *Regional to wellbore analog for fluvial-deltaic reservoir modeling; the Ferron Sandstone of Utah*, **50**, pp. 59-78. American Association of Petroleum Geologists, Tulsa, OK, United States.

Skorstad, A., Kolbjørnsen, O., Manzocchi, T., Carter, J.N. and Howell, J.A. (2008) Combined effects of structural, stratigraphic, and well controls on production variability in faulted shallow marine reservoirs. *Petroleum Geoscience*, **14,** 45-54

Stephen, K.D., Yang, C., Carter, J.N., Howell, J.A., Manzocchi, T. and Skorstad, A. (2008) Upscaling uncertainty analysis in a shallow-marine environment. *Petroleum Geoscience*, **14,** 71-84

Tye, R.S., Bhattacharya, J.P., Lorsong, J.A., Sindelar, S.T., Knock, D.G., Puls, D.D. and Levinson, R.A. (1999) Geology and stratigraphy of fluvio-deltaic deposits in the Ivishak Formation; applications for development of Prudhoe Bay Field, Alaska. *AAPG Bulletin*, **83,** 1588-1623

van den Bergh, T.C.V. and Garrison, J.R. (2004) The geometry, architecture, and sedimentology of fluvial and deltaic sandstones within the upper Ferron Sandstone Last Chance Delta; implications for reservoir modeling. In: *Regional to wellbore analog for fluvial-deltaic reservoir modeling; the Ferron Sandstone of Utah*, **50**, pp. 451-498. American Association of Petroleum Geologists, Tulsa, OK, United States.

Van Wagoner, J.C., Mitchum, R.M., Campion, K.M. and Rahmanian, V.D. (1990) *Siliciclastic Sequence Stratigraphy in Well Logs, Cores, and Outcrops: Concepts for High-Resolution Correlation of Time and Facies*. American Association of Petroleum Geologists, 55 pp.

Weber, K.J. (1986) How heterogeneity affect oil recovery. In: *Reservoir characterization* (Eds L.W. Lake and H.B. Carroll), pp. 487-544. Academic Press, Orlando.

Weber, K.J. and van Geuns, L.C. (1990) Framework for constructing clastic reservoir simulation models. *Journal of Petroleum Technology*, **42,** 1248-1253, 1296-1297

White, C.D. and Barton, M.D. (1999) Translating outcrop data to flow models, with application to the Ferron Sandstone. *Society of Petroleum Engineers Journal, Paper No. 38741*, 233-248

Willis, B.J. and White, C.D. (2000) Quantitative outcrop data for flow simulation. *Journal of Sedimentary Research*, **70,** 788-802

Young, R.G. (1955) Sedimentary interfacies and intertonguing in the Upper Cretaceous of the Book Cliffs, Utah-Colorado. *Geological Society of America Bulletin*, **66,** 177-201